water

MDPI

Article

Hydro-Meteorological Characterization of Major Floods in Spanish Mountain Rivers

Enrique Morán-Tejeda [1,2,3,*], Steven R. Fassnacht [2,3,4], Jorge Lorenzo-Lacruz [5], Juan Ignacio López-Moreno [6], Celso García [1], Esteban Alonso-González [6] and Antonio-Juan Collados-Lara [2,3,7]

1 Department of Geography, University of the Balearic Islands, Palma 07122, Spain; celso.garcia@uib.es
2 ESS—Watershed Science, Colorado State University, Fort Collins, CO 80523, USA; Steven.Fassnacht@colostate.edu (S.R.F.); aj.collados@igme.es (A.-J.C.-L.)
3 Natural Resources Ecology Laboratory, Colorado State University, Fort Collins, CO 80523, USA
4 Cooperative Institute for Research in the Atmosphere, Colorado State University, Fort Collins, CO 80523, USA
5 Department of Human Sciences, Physical Geography University of La Rioja, Logroño 26004, Spain; jorge.lorenzo@unirioja.com
6 Pyrenean Institute of Ecology, Spanish Research Council (CSIC), Zaragoza 50059, Spain; jlopez@ipe.csic.es (J.I.L.-M.); e.alonso@ipe.csic.es (E.A.-G.)
7 Department of Research on Geological Resources, Geological Survey of Spain, 18006 Granada, Spain
* Correspondence: e.moran@uib.es

Received: 12 November 2019; Accepted: 10 December 2019; Published: 14 December 2019

Abstract: Spain, one of the most mountainous countries in Europe, suffers from frequent river flooding due to specific climatic and topographic features. Many headwaters of the largest rivers in Spain are located in mountainous areas of mid-to-high elevation. These include the Pyrenees, the Central System, and the Cantabrian mountains, that have a sustained snowpack during the winter months. Most previous research on flood generation in Spain has focused on intense rainfall events, and the role of snowmelt has been ignored or considered marginal. In this paper we present a regional-scale study to quantify the relative importance of rainfall versus snowmelt in the largest floods recorded in mountain rivers in Spain during the last decades (1980–2014). We further analyzed whether catchments characteristics and weather types may favor the occurrence of rainfall or snowmelt induced floods. Results show that in 53% of the 250 analyzed floods the contribution of rainfall was larger than 90%, and in the rest of events snowmelt contribution was larger than 10%. Floods where snowmelt was the main contributor represented only 5% of the total events. The average contribution of snowmelt represents 18% of total runoff in floods that were analyzed. The role of snowmelt in floods, rather than triggering the event, was usually amplifying the duration of the event, especially after the peak flow was reached. In general, the importance of snowmelt in floods is greater in catchments with characteristics that favor snow accumulation. However, this does not apply to floods where contribution of snowmelt was larger than 90%, which tend to occur at catchments at mid-elevations that accumulate unusual amounts of snow that melt rapidly. Floods were more frequent under both cyclonic and anticyclonic synoptic situations over the Iberian Peninsula, as well as under advection of western and eastern flows. Our results contribute to the ongoing improvement of knowledge about the role of snow in the hydrology of Spanish rivers and on the importance of mountain processes on the hydrology of downstream areas.

Keywords: floods; rain; snowmelt; rain-on-snow; Spanish mountains; weather types

1. Introduction

Mountains are important for water resources across the world [1]. They constitute the headwaters of major fluvial systems, storing water in the form of snow, ice, groundwater, or lakes. Both the quantity and the timing of water flowing downstream depend on the elevation, drainage area, and other geographical characteristics of mountains. However, due to complex topography and large elevation gradients, the same mechanisms involved in the generation of water may create major risks, such as landslides, avalanches, and floods. Mountains facilitate adiabatic uplift of air masses, and convective precipitation [2] and the steep slopes enable surface runoff and rapid water routing, increasing the potential for flood generation [3,4]. Greater damage to society usually occurs downstream, where most of the population is concentrated, and where water from different tributaries converges in the main stream, causing a substantial increase in streamflow and potential risk.

Flooding in mountain areas shows a seasonal distribution and elevation dependence, as does the generation of runoff. They both depend on the consolidation of the snowpack during the winter season and further melting when temperatures increase. Weingartner et al. [4] showed across the European Alps that the likelihood for intense floods is greatest for catchments located between 1000 m and 2000 m. Below the 1000 m limit, less intense precipitation, deeper soils, or more vegetation reduce runoff intensity. Above 2000 m, a large proportion of precipitation accumulates in the snowpack, reducing the magnitude of floods. However, such a framework assumes that intense rainfall is the sole source of water for flooding. While that can be true for warm climates, in regions with a regular presence of snow, such as mountains or boreal latitudes, snowmelt runoff can also be an important source of river flooding [5,6]. In mid-latitude mountain areas warm temperature events with associated rainfall can occur in winter and more often in spring, inducing runoff generation from combined snowmelt and rainfall. Rain-on-snow (ROS) events are defined as the hydro-meteorological events in which liquid rain falls on the snowpack and have been often described in the literature [7,8]. The warmer than freezing air temperature that causes precipitation to fall in a liquid state may melt snow, and that meltwater combined with the water from rainfall can trigger increased surface runoff and as a consequence flooding. While a ROS does not necessarily generate river flooding, major floods associated with ROS have been reported in the mountains of Western United States [9,10], in Southern Germany [11], Switzerland [12], Austria [13], the Spanish Pyrenees [14], or the Canadian Rockies [15]. Morán-Tejeda et al. [16] demonstrated the relevance of elevation and seasonality for ROS to occur; in Switzerland they peak at elevations between 800–1200 m in winter and between 1800–2600 m in spring and summer, highlighting the importance of considering snowmelt, together with the amount of rain, when forecasting river flooding in mountain areas.

Floods are considered as the most damaging environmental risk in Spain in both socio and economic terms [17]. More than 20 floods per 10,000 km^2 were registered between 1980 and 2015, one of the highest rates in Europe, that accounted for 652 fatalities [18]. The complex Spanish topography, along with the Atlantic–Mediterranean transition climatic features, leads to frequent events of intense precipitation with the potential of generating floods on a yearly basis [19]. Major precipitation events that generate floods in Spain are mainly triggered by two atmospheric configurations: (i) Advection of Atlantic frontal systems, with long persistent rainfalls affecting the river basins in the western half of the country [20], and (ii) heavy convective storms induced by the advection of cut-off-lows (i.e., a cold depression in the mid troposphere originated from the detachment of cold air with cyclonic vorticity from the subpolar circulation that usually heads to mid-latitudes) and warm sea surface conditions, and boosted by orographic uplift [21]. The latter storms cause the so-called flash-floods and are more usual in the small river catchments of the eastern Mediterranean façade [22,23].

Continental Spain has a mean elevation of 600 m a.s.l., with several mountain systems depicting permanent winter snowfields and an important contribution of snow to the hydrological cycle [24–27]. The hydrological role of snow in Spanish mountains has been receiving scientific attention over the last two decades [26–29]. However, the role of snowmelt on the amplification of the damaging nature of floods has been considered marginal, or has not received proper evaluation [19,30]. This is in part

due to the difficulty in quantifying the volume of snow accumulated in the mountains and its water content. Only recently has attention been put on the role of snowmelt, due to the damaging floods that have occurred in the Ebro River during warm spells over the last two decades [14,31]. This was thanks to techniques that allow a reasonable estimation of the quantity of water in the snowpack, including remote sensing and modeling approaches. On this regard, a new range of possibilities for research on snow hydrology in Spain was recently opened up with the publication of a gridded dataset of snow depth and snow water equivalent for Spain by Alonso-González et al. [32].

Considering the abovementioned research gap and the new snow dataset for the Spanish mountains [32], the aim of this paper is to determine the main drivers of major floods in mountain rivers in Spain. Specifically, the objectives of the research are (1) to determine whether the major floods are derived from rain, snowmelt, or a combination of rain and snowmelt; (2) to quantify the relative contribution of each on the total flooding streamflow; (3) to explore the main characteristics of the floods hydrographs [27,28] according to the relative contribution of rainfall and snowmelt and (4) to determine whether the geographical characteristics of the catchments, and atmospheric circulation over the Iberian region can explain the relative importance of rainfall and snowmelt in triggering major floods.

2. Methods

2.1. Data

Daily streamflow data from 25 mountain river streams (Table 1 and Figure 1c) were obtained from the Spanish Center for Studies and Experimentation on Public Works (CEDEX in Spanish), within the Spanish Ministry of Development, freely available at [33]. All streams had a maximum watershed elevation higher than 1500 m a.s.l., to ensure mountain climatic characteristics, specifically frequent snowfalls and/or the presence of seasonal snowpack, and the absence of any artificial infrastructure that would alter the natural regime of the river flows.

Table 1. Mountain rivers selected for the study (ordered by gauge elevation), and their main characteristics.

ID	River	Mountain System	Gauge Elevation (m a.s.l.)	Max Elevation (m a.s.l.)	Drainage Area (km^2)	Mean Daily Flow ($m^3\ s^{-1}$)	Mean Annual Specific Discharge ($L\ s^{-1}\ km^{-2}$)	Largest Flood Flow ($m^3\ s^{-1}$)
1196	Asón	Cantabrian Range	16	1640	512	21.3	411.5	793.5
1207	Miera	Cantabrian Range	50	1707	166	4.6	265.0	306.9
1268	Deva	Cantabrian Range	56	2536	643	13.0	201.8	540.0
1363	Caudal	Cantabrian Range	352	2386	232	5.6	226.9	183.4
1353	Narcea	Cantabrian Range	352	2007	531	15.8	290.1	241.4
9013	Ésera	Pyrenees	450	3404	893	17.1	186.6	330.8
9050	Tirón	Iberic System	526	2085	698	3.8	54.4	119.7
9022	Valira	Pyrenees	559	2865	559	8.6	150.8	123.4
9152	Arga	Pyrenees	582	1459	69	2.5	354.4	74.6
9023	Segre	Pyrenees	670	2921	1233	12.0	92.1	213.4
9040	Ara	Pyrenees	680	3355	626	16.1	250.8	651.6
9066	Irati	Pyrenees	700	2021	236	9.7	403.0	293.6
9018	Aragón	Pyrenees	793	2886	238	5.4	227.1	206.0
2057	Pirón	Cantabrian Range	869	2200	172	0.7	35.0	34.0
2012	Duratón	Central System	920	2262	480	1.9	37.5	57.2
2016	Cega	Cantabrian Range	938	2209	280	2.5	88.6	67.6
9044	Cidacos	Iberian System	940	1792	223	1.2	51.7	48.9
5086	Dilar	Baetic System	957	3392	41	1.1	267.7	31.5
9043	Linares	Iberian System	1060	1709	105	0.4	41.6	9.2
2068	Curueño	Cantabrian Range	1094	2067	154	4.4	276.2	109.0
2101	Duero	Iberian System	1100	2015	135	2.4	176.5	166.7
2009	Riaza	Central System	1139	2036	36	0.5	141.8	10.5
9080	Veral	Pyrenees	1187	2366	47	1.5	316.6	28.5
2034	Besandino	Central System	1270	1820	32	1.3	401.2	23.3
2006	Tormes	Central System	1377	2592	88	1.5	158.3	45.2

Meteorological surface data was derived from the ERA-Interim reanalysis dynamically downscaled to 10 × 10 km resolution with the Weather Research and Forecasting model (WRF) by García-Valdecasas

et al. [34]. This was then coupled with a snow energy-balance simulation with Factorial Snow model (FSM), by Alonso-González et al. [32]. They used the downscaled climate data to run the FSM and constructed a semi-distributed grid of daily snow depth (SD) and snow water equivalent (SWE) with 10×10 km resolution for the entire Iberian Peninsula spanning from 1980 to 2014. The grid was vertically rescaled to 100 m elevation bands using an array of radiative and psychrometric formulas and lapse rates (see details in [32]). Alonso-González et al. [32] proved the consistency of the database with in situ SD and SWE observations and remote sensing data, accurately reproducing the temporal and spatial patterns of snow. For the purpose of our study, we extracted both, the downscaled climate data (3-hourly temperature, relative humidity and precipitation) and the daily SWE data corresponding to the extent of the 25 selected river watersheds.

2.2. Data Processing and Analysis

From the 25 selected streams, we picked the 10 largest floods in the period 1980–2014, based on the 10 largest values of daily flow for individual events. We computed the return period for each peak flow value (χ) by adjusting the series of maximum daily flow per year from the General Extreme Value (GEV) distribution (a standard tool for modeling flood peaks [35,36]) and computing the inverse of the probability of finding a value larger than χ, using:

$$RT = \frac{1}{1 - F(\chi)}$$

where RT is the return period, and $F(\chi)$ is the empirical cumulative distribution for GEV function for χ.

As observed in Figure 1a, the return periods for the largest event of each river are in the range of 20 years to 80 years, they drop to 15 years for the 3rd largest event, and around 1–2 years from the 5th largest event and beyond. As such, we selected 10 events per river, as more events per station would not add any other large events for our analysis. For the 250 events, we selected a 31-day window of streamflow data, with the peak flow in the center (16th day). Then we visually identified the beginning (when the flow starts rising) and end (when the flow is back to baseflow) day of the flood event, from the daily flow and the cumulative flow time series for the 31-day flood event window.

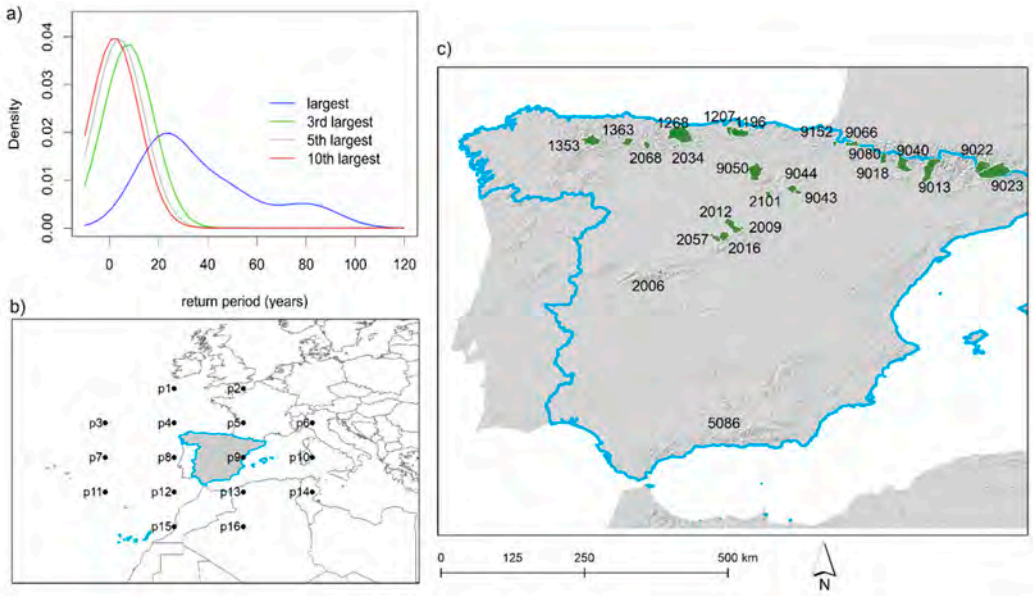

Figure 1. (**a**) Frequency distributions of return periods for the first, third, fifth and tenth largest flood events in each of the 25 studied rivers. (**b**) Map of Western Europe, with grid points used for calculation of indices that define weather types according to Table 4. (**c**) Map of Spain with locations of catchments of the studied mountain rivers and their ID code (Table 1).

Precipitation and SWE data were extracted from the WRF and FSM simulations performed by Alonso-González et al. [32] and were further used to compute the relative weight of rainfall and snowmelt on the generation of floods. A snowmelt event was defined as the day in which the SWE value was lower than the value of the previous day; the difference of the two values was then considered as the quantity of snowmelt on such day. Then for each 3-hourly precipitation record, rainfall events were isolated from snowfall events by computing the precipitation phase (rainfall/snowfall) for each 100-m elevation band. This was calculated using the psychometric energy balance model detailed in Harder and Pomeroy [37] with temperature and relative humidity changing as a function of elevation. Once the rainfall and snowmelt values per elevation band were isolated, we computed, for each flood event, the cumulative sums from the day when the event started, to the day of the peak flow. On the base of such cumulative values, we calculated, for each flood event, the rain/snowmelt ratio (R/S) as the amount of rainfall relative to the sum of cumulative rainfall and meltwater from the day of beginning of the event to the day of the peak flow. This ratio allowed us defining each flood event as follows: Rain event (hereafter *rain*), when the R/S was larger than 0.9; rain-on-snow with prevalence of rain (*ROS_r*), when R/S was between 0.75 and 0.9; rain-on-snow (*ROS*) when R/S was between 0.25 and 0.75; rain-on-snow with prevalence of snow (*ROS_s*) when R/S was between 0.1 and 0.25; and snowmelt event (*snow*) when the R/S was smaller than 0.1.

We then explored the characteristics of hydrographs for each type of flood to discern whether the relative contribution of rainfall and snowmelt involve different shapes in the flood hydrograph. For this we computed a number of indices from the streamflow between the start and end of the event, namely: Magnitude, total flow, duration, slope of the rising limb (SRiL), slope of the receding limb (SReL), and day of hydrological year of the peak flow (DHY) (see explanation of indices in Table 2).

Table 2. Indices used for defining the hydrographs.

Index	Definition	Unit
magnitude	difference between the peak flow value and the flow value at the beginning of the event	mm day^{-1}
total flow	area under the flow curve between the beginning and end of the event	mm day^{-1}
duration	number of days between the beginning and end of the event	number of days
SRiL	slope of the flow between the beginning day and the day of peak flow	Δ flow/Δ time
SReL	slope of the flow between the day of peak flow and the ending day	Δ flow/Δ time
DHY	day of the hydrological year (from 1 October to 30 September) when the peak flow occurred	day of year

Similarly, to explore the geographical influence on the role of rainfall and snowmelt on the generation of floods, we computed a number of indices that define the topographic and climatic characteristics of the catchments: Mean radiation which is indicative of the exposure of the catchments' slopes; hypsometric index as a relative measure of area vs. elevation; average temperature; winter–spring precipitation and summer–fall precipitation; extreme precipitation index—Epi—for the December-to-May, and June-to-November semesters (winter–spring EPi and summer–fall EPi); days with snow, and peak SWE (see explanation of each index in Table 3).

Table 3. Characteristics of the catchments where studied flood occurred. * Hypsometric index was computed for each catchment by multiplying the elevation of each 100 m elevation band from 500 m to 2900 m by the relative area in each band, and computing the average of all the resulting values; low (high) values indicate small (large) areas covering high elevations.

Index	Definition	Unit
area	drainage area extension	km^2
mean radiation	mean daily solar radiation values, averaged from 10 × 10 m pixels	w m^2
hypsometric index *	relative measure of area vs elevation	-
average T	long-term annual mean temperatures	°C
winter–spring P	long-term average of cumulative precipitation for December-to-May	mm
summer–fall P	long-term average of cumulative precipitation for June-to-November	mm
extreme precipitation index–EPi	number of days with precipitation larger than the 90th percentile relative to the total precipitation days	days
days with snow	long-term average of the number of days per year with SWE value larger than 1 mm	days
peak SWE	long-term average of the largest SWE value per year	mm

2.3. Weather Types

We further explored the atmospheric circulation over the Iberian Peninsula when the 250 flood events occurred. For this, we adopted the weather types characterization proposed for Trigo and DaCamara [38], that is based on the objective classifications for the British Islands proposed by Jenkinson and Collison [39] and Jones et al. [40]. This classification has been successfully used in studies about climate variability and precipitation over the Iberian region [41–43]. The daily circulation weather types are based on a set of indices that quantify the direction and vorticity of geostrophic flow, namely: Southerly flow (SF), westerly flow (WF), total flow (F), southerly shear vorticity (ZS), westerly shear vorticity (ZW), and total shear vorticity (Z) (Table 4). These indices were calculated using daily sea level pressure (SLP) values from 16 grid points with longitude—latitude resolution of 10° × 5°, centered over the Iberian Peninsula, as in Cortesi et al. [44] (Figure 1b). Daily SLP data from 1980–2014 was obtained from the NCEP/NCAR Reanalysis, and the indices were computed for the day of beginning of the 250 flood events, as indicated in Table 4.

Table 4. Computation of indices used for weather types characterization. p1–p16 points are depicted in Figure 1b.

Direction and Vorticity Indices	Abbreviation	Computation
southerly flow	SF	1.305 [0.25 (p5 + 2p9 + p13) − 0.25 (p4 + 2p8 + p12)]
westerly flow	WF	[0.5 (p12 + p13) − 0.5 (p4 + p5)]
southerly shear vorticity	ZS	0.85 [0.2 (p6 + 2p10 + p14) − 0.25 (p5 + 2p9 + p13) − 0.25 (p4 + 2p8 + p12) + 0.25 (p3 + 2p7 + p11)]
westerly shear vorticity	ZW	1.12 [0.5 (p15 + p16) − 0.5(p8 + p9)] − 0.91 [0.5 (p8 + p9) − 0.5 (p1 + p2)]
total flow	F	0.5 (SF2 + WF2)
total shear vorticity	Z	ZS + ZW

Given indices in Table 4, the weather types are defined based on the following criteria:

1. Flow direction is given by $tan^{-1}\left(\frac{WF}{SF}\right) 180/\pi$, results in sexagesimal degrees. 180° were added if WF > 0. The corresponding direction (N, NE, E, SE, S, SW, W, NW) is then computed using an eight-point compass, allowing 45° per sector.
2. If |Z| < F, flow is essentially straight and weather type can be considered as advective or pure directional type (eight different cases according to the compass directions).
3. If |Z| > 2 F, the weather type is considered as pure cyclonic when Z > 0, and pure anticyclonic when Z < 0.
4. If F < |Z| < 2 F, the flow is considered to be a hybrid type, characterized by both direction (rule 1) and circulation (rule 3) (8 × 2 different types).

The classification results then in 26 weather types, including 8 pure advection types, 2 pure circulation types, and 16 hybrid types. However, in order to simplify representation of results, the 26 weather types were re-grouped into 10 basic ones following Trigo and DeCamara [38]. For this, each of the 16 hybrid types was included with a weight of 0.5 into the corresponding directional and cyclonic/anticyclonic types (e.g., one case of cyclonic SW was included as 0.5 in cyclonic and 0.5 in SW). The days when floods of interest occurred were classified as one of the 10 basic types, so we knew the type of atmospheric configuration that lead to the occurrence of the flood.

3. Results

3.1. Hydrological Drivers of Flood Events

Results of quantification of the relative role of snowmelt and rain on flood generation (Figure 2a,b) shows that 53% of the large flood events were caused mainly by rainfall, 2.5% of events were caused by only snowmelt, and the remaining 45.5% by a combination of rainfall and snowmelt. Of the ROS flood events, 23% were caused by a ROS with quantity of rainfall larger than the quantity of snowmelt (*ROS_r*), with 19% where rainfall and snowmelt contributed in a similar amount (*ROS*); and only 2.5% with a larger contribution of snowmelt than rainfall (*ROS_s*). The classification of events by river (Figure 2c) does not have an obvious spatial pattern, but we do observe that the relative quantities of events by hydrological driver commented above, changes notably from one river to another. The average value of the R/S ratio amongst the 250 events is 81.9 (dashed line in Figure 2b). Therefore, snowmelt generates on average 18% of the total bulk water for floods in Spanish mountain rivers.

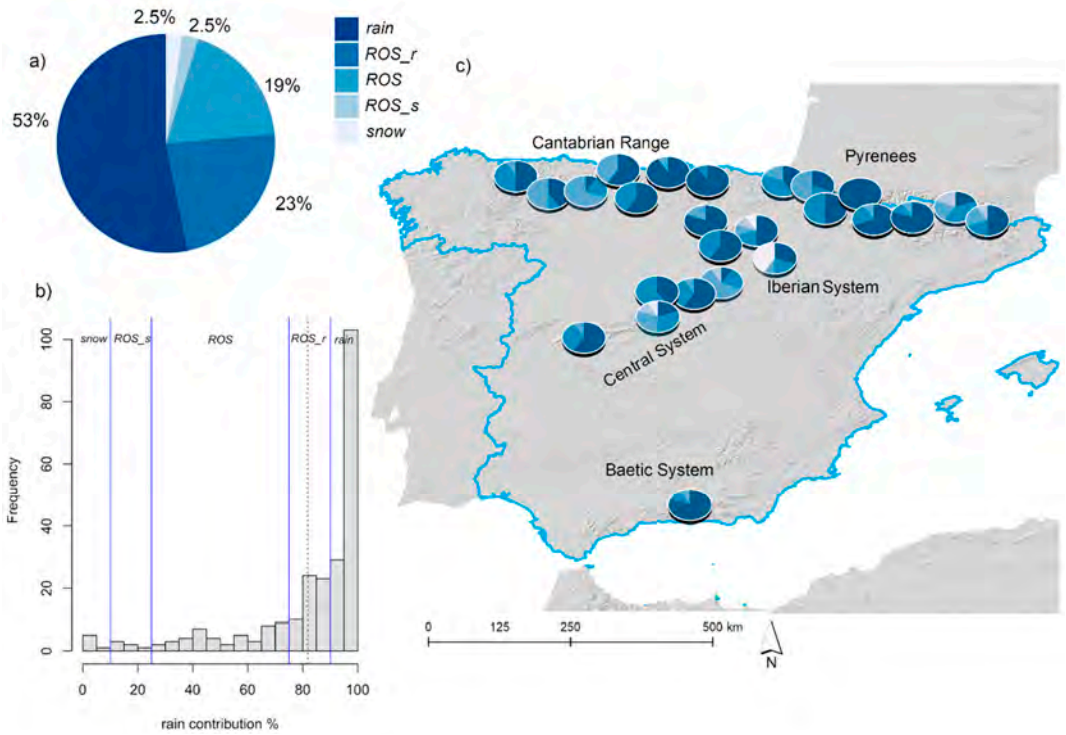

Figure 2. (**a**) Percentage of flood events by type for the entire 250 sample of events. (**b**) Frequency of events by contribution of rain, with blue lines indicating thresholds for classifying type of floods and dashed line indicating mean rain contribution for all events 9. (**c**) Map of Spain with location of studied rivers and the percentage of flood events by type for the 10 events in each individual river. Color legend in 9 (**a**) is valid for (**c**).

We observe differences in the relative importance of snowmelt when events are categorized by magnitude (Figure 3b). For the largest (Figure 3a) and second largest floods amongst all rivers,

the number of events with participation of snowmelt is slightly larger than the number of *rain* events (52% vs. 48%); this is also true for the 8th and 10th greatest events. Conversely, events ranked third-to-seventh and ninth were predominantly driven by rainfall (Figure 3b). We observe that in the Pyrenees (northeastern Spain), the largest floods have been mainly caused by rainfall, whereas in the western mountain rivers most of the largest floods had an important contribution of snowmelt (Figure 3a). Interestingly, in the two rivers located in the Iberian System that drain into the Ebro basin (Cidacos and Linares Rivers), the largest studied floods were generated by snowmelt. As well, of the five floods with a return period of more than 90 years (Figure 1), three of them are *ROS_r* events, and the other two are *rain* events (Figure 3b).

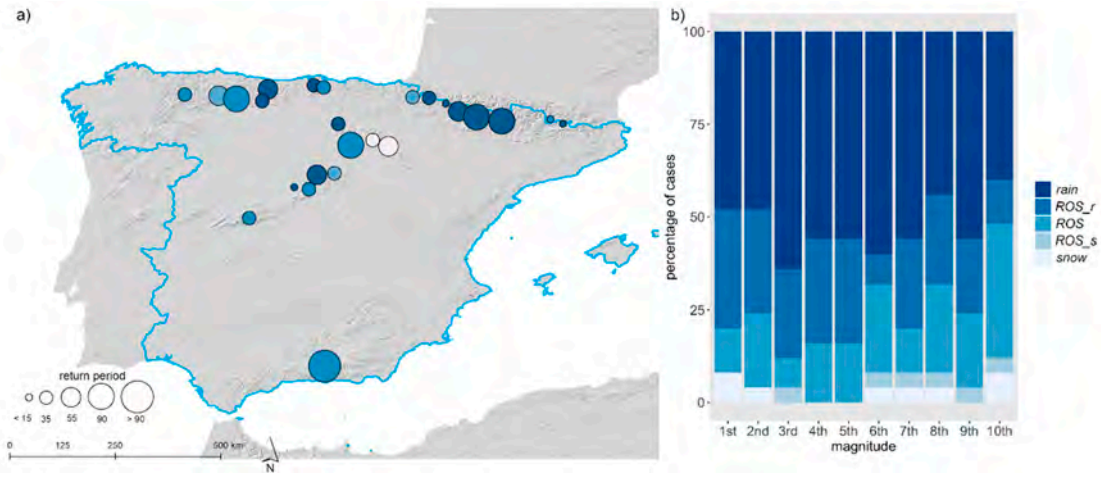

Figure 3. (**a**) Map of the category (color) of the largest flood event in each river and the return period of the event (size). (**b**) Bar chart shows the percentage of flood events of each category, ordered from left to right by their magnitude.

Flood events in mountain rivers depict a clear seasonal pattern (Figure 4). Winter months (December through February) account for the 45.5% of total events, whereas spring and fall account for 27% and 20% of events respectively (Table 5). But when it comes to the monthly distribution of events by hydrological driver, the seasonality is even larger: of the total number of events in winter, 33% were *rain* floods, while in the remaining 67%, snowmelt played a role. In spring, there is similar number of events induced by only rain (53.7%) and induced by rain and snowmelt (46.3%). The number of events triggered by rain increases in summer and fall to 74% and 90% respectively. Events where snow was the main driver of flooding occurred only in winter months (Figure 4 and Table 5).

Table 5. Percentage of flood events by season and hydrological driver category. Winter includes December, January and February; Spring includes March, April and May; Summer includes June, July and August; and Fall includes September, October and November.

Season	*Rain*	*ROS_r*	*ROS*	*ROS_s*	*Snow*
Winter	33.6	28.3	29.2	3.5	5.3
Spring	53.7	25.4	20.9	0.0	0.0
Summer	73.7	10.5	15.8	0.0	0.0
Fall	89.8	8.2	2.0	0.0	0.0

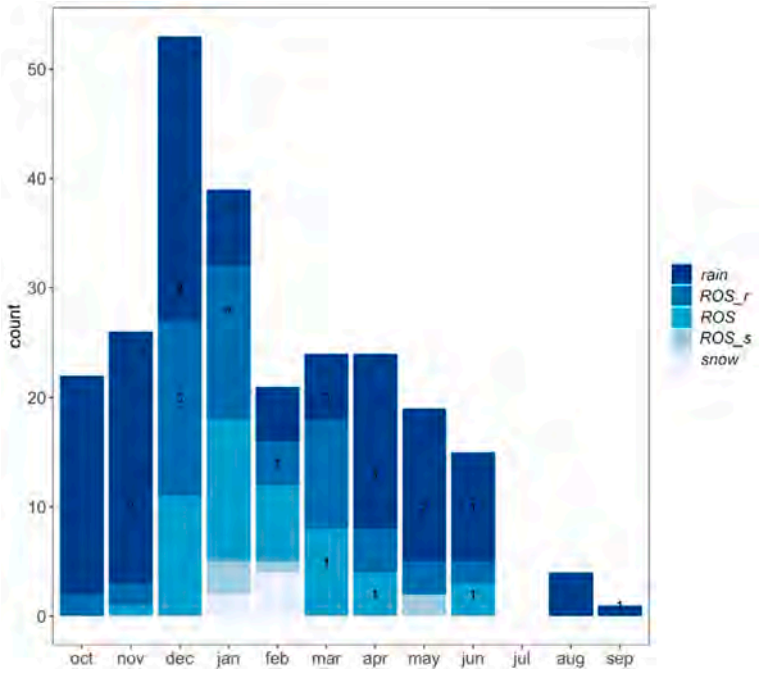

Figure 4. Number and category of flood events by month (ordered according to hydrological year). Figures inside bars indicate the number of times that the greatest flood occurred by month and category.

3.2. Characteristics of Hydrographs by Flood Type

The various flood types have different hydrographs (Figure 5), but with a common pattern based on the relative role of snowmelt in the generation of the event. *Rain* floods are observed throughout the entire hydrological year (see large box and whiskers in boxplot) but generally tend to occur in fall and early winter days (see median line in boxplot around Julian day 90, i.e., late December). On the contrary, floods with a snowmelt contribution occur later, and the more contribution of snow, the later they tend to occur (late winter days) (Figure 5). The slope of the rising limb informs of the rate at which the peak flow is reached from the beginning of the event. We observe that as the contribution of snowmelt increase, the longer it takes to reach peak flow, i.e., a lower slope. The same pattern is observed in the slope of the receding limb, i.e., from peak flow until the end of the event. This indicates that floods with a contribution of snowmelt are less sudden in their generation, and tend to stay longer after the peak flow is reached. This is further seen by the pattern observed in the duration of the events, which is longer when the contribution of snowmelt is bigger.

The mean duration of floods is about 15–16 days, with very few cases (7) lasting less than 5 days, confirming that flash-floods are rare events in the Spanish mountains or did not reach a magnitude enough as to be included in our study. Finally, when examining the magnitude of the event (how high is the peak flow with respect to baseflows), we observe that the largest peak flows are generally reached in *rain* events, although some *ROS* events may also reach comparable magnitudes (see longitude of the whiskers depicting the 95th percentiles). However, when examining the total flow generated during the flood, we observe that events with a contribution of snowmelt produce more (*ROS_r*), or similar (*ROS*) flow volume than *rain* events (note that flow volume is expressed in mm day^{-1} in order to make values independent of catchment size). *Snow* floods (which are very few in number) show both the smallest magnitude and volume of flow.

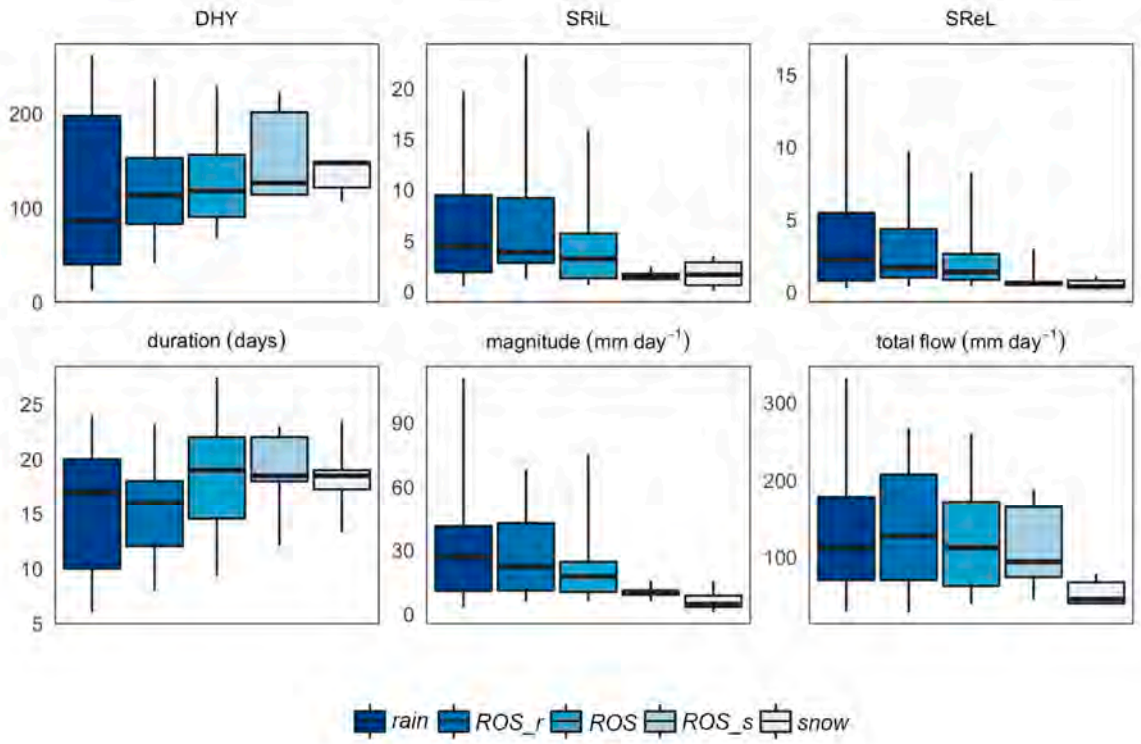

Figure 5. Distributions of values of hydrographs characteristics for the different types of floods. Solid line indicates the median, boxes the first and third quartiles, and whiskers the 5th and 95th percentiles. n (*rain*) = 133; n (*ROS_r*) = 58; n (*ROS*) = 47; n (*ROS_s*) = 6, n (*snow*) = 6. "Magnitude" and "total flow" are expressed in mm day^{-1} (result of multiplying streamflow in m^3 s^{-1} by the number of seconds in a day, and dividing by the extension of the catchment) in order to make values independent of catchment size, therefore comparable. DHY: Day of the hydrological year when the peak flow occurred; SRiL: slope of the rising limb; SReL: slope of the receding limb (see Table 2).

3.3. Geographical Drivers of Flood Type

Since no clear spatial pattern was found in the distribution of floods by hydrological driver (Figure 2), we examined if topographic and climatological characteristics of the catchments can explain the prevalence of flood type (Figure 6). The low variability of *snow* events is due to this type of flood only occurring 6 times, and in three catchments, two of them with very similar characteristics (Figure 6). No clear differences are observed between flood types due to the catchment area and mean daily solar radiation, which is indicative of the predominant exposure of the catchment slopes. The hypsometric index is a relative measure of the quantity of area per elevation band, and we only observe a significant difference in *ROS_s* compared to the other flood types; these tend to occur in catchments with more area at higher elevations. A similar pattern is observed for the temperature per catchment since it is related to the hypsometry; *ROS_s* floods occur predominantly in catchments with lower temperatures while the few numbers of snow floods recorded occurred in catchments with higher temperatures.

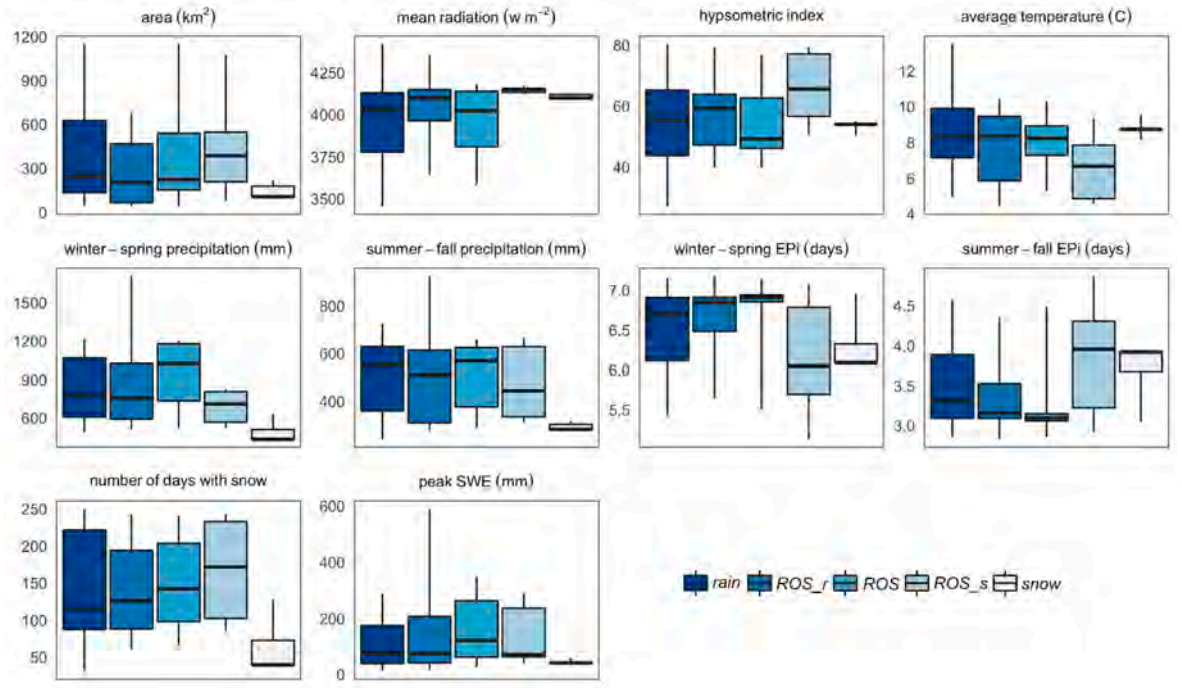

Figure 6. Distributions of values of topographic and climatological indices for the catchments where the different types of floods occurred. Solid line indicates the median, boxes the first and third quartiles, and whiskers the 5th and 95th percentiles. n (*rain*) = 133; n (*ROS_r*) = 58; n (*ROS*) = 47; n (*ROS_s*) = 6, n (*snow*) = 6. EPi: Extreme Precipitation index (see Table 3).

We observe a different pattern depending on the seasonal aggregation of precipitation considered. For winter–spring precipitation, *ROS* floods, tend to happen in catchments with a larger cumulative precipitation, and *ROS_s* and *snow* floods in catchments with less total precipitation. For summer–fall precipitation, the only type of floods with a differentiated behavior are *snow* floods, but this is not relevant since this type of flood does not occur on summer or fall months. When considering the importance of extreme precipitation events (EPi, see Table 3) by catchment we also observe a different behavior of floods types and seasonal aggregation: winter–spring EPi (summer–fall EPi) is higher (lower) in catchments where *rain*, *ROS_r* and *ROS* prevail and significantly lower (higher) in catchments where *ROS_s* and *snow* events predominate. This clearly indicates the different nature of climate in catchments where snowmelt driven floods prevail, compared to the catchments with more abundant rain-dominated floods. Another noticeable difference, perhaps the most obvious pattern, is for snow-related indices. Excluding *snow* floods with an anomalous behavior, and considering the large variability amongst cases (large boxes and whiskers), we generally observe that the more days with snow, and the larger the peak SWE in the catchment, corresponds to a larger contribution of snowmelt for a flood.

3.4. Atmospheric Circulation and Floods

The mountain rivers that we examined may flood under any type of weather types, although some weather types show more importance than others (Figure 7). The most often circulation pattern that caused floods was cyclonic weather type (67 cases, 26%). Floods also occurred under anticyclonic conditions but in fewer cases (21 cases, 7%). The advective conditions more favorable for flood occurrence are flows from SW and W, which account together a 26% of cases, as well as E and SE flows, with a 22% of cases (Figure 7a). *Rain* floods are the most common events during cyclonic, W and SW weather types. Conversely, during advective conditions from the E and SE, a majority of the floods have a contribution from snowmelt. In Figure 7b we observe that *rain*, *ROS_r* and *ROS* floods, which occur most often (Figure 2a), can happen under almost any type of low atmosphere configuration, albeit with

certain differences: For *rain* floods the most common weather type is cyclonic; for *ROS_r*, *ROS*, and *ROS_s* floods, cyclonic, and advection from SE and E prevail; and *snow* floods occurred under cyclonic, SW and W conditions. The latter lacks, however, statistical significance, due to the low number of events (6) recorded. Finally, when grouping events by mountain system (Figure 7c), the pattern above described—cyclonic and advection from SW and SE—prevails across most of them, although small differences exist. For example, in the Pyrenees, 14% of floods occurred under anticyclonic circulation and in the Baetic System, with only one river sampled (10 events), the predominant weather types for flood occurrence were anticyclonic, cyclonic, and advection from NW.

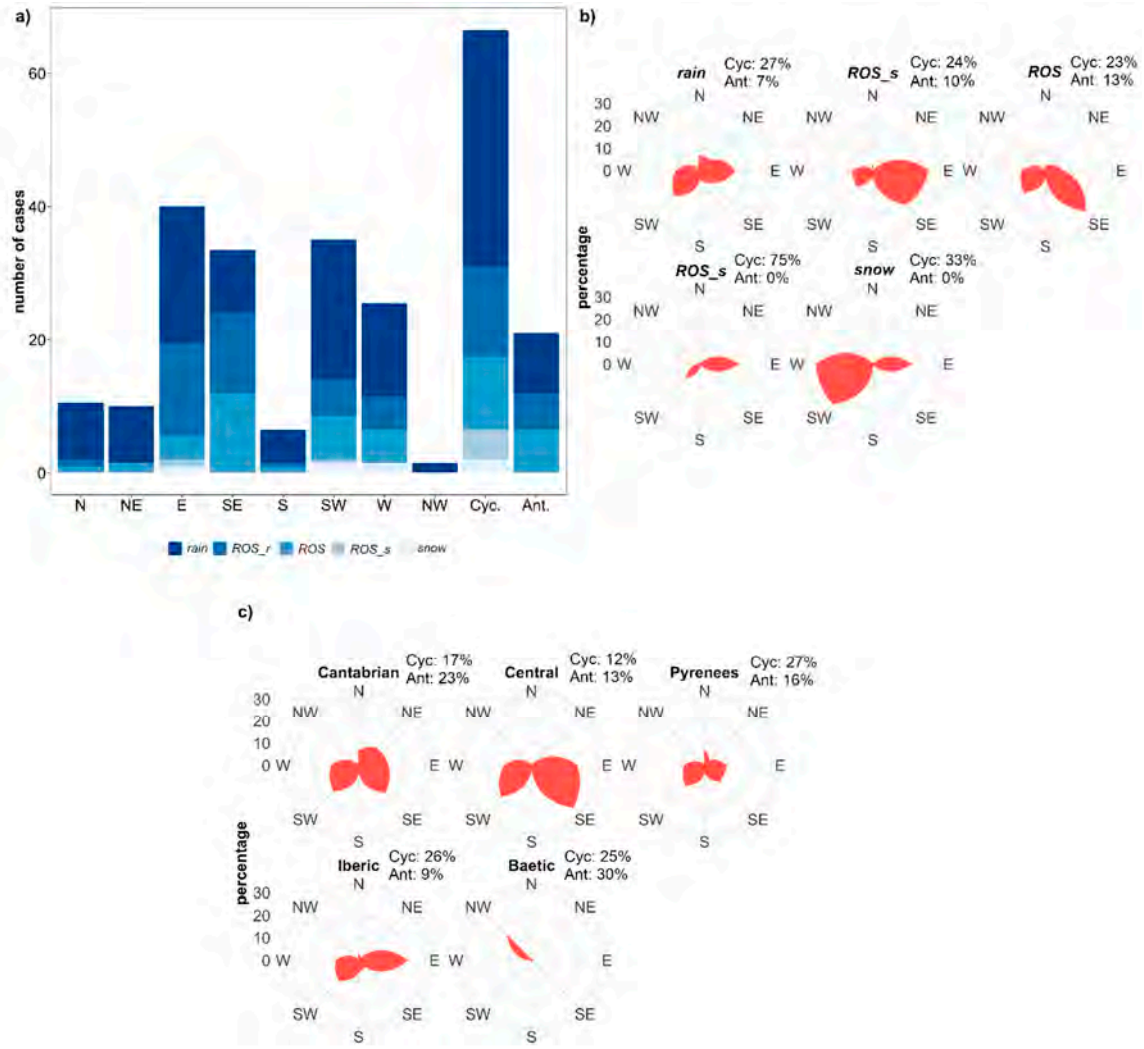

Figure 7. Weather types during floods. (**a**) Number of floods by weather type, (**b**) percentage of weather types for each type of flood, AND (**c**) percentage of floods by weather type and mountain system.

3.5. A Case Study: Floods Aggregation Downstream

In this last section we present a case study that helps visualize the cause of flood generation, the role of rainfall and snowmelt, and highlights the importance of floods in mountain tributaries when aggregating in downstream main river courses. Of the 250 studied events, we selected, as an example, a flood on 18 December, 1997, because it occurred concurrently in 8 Pyrenean catchments (see example of three catchments at Figure 8) that belong to the Ebro River watershed. Based on the weather type classification, pure cyclonic circulation conditions existed over the Iberian Peninsula, which lead to a 72-h precipitation event over the Pyrenees. We observe that the 72-h precipitation fell in the form of snow at high elevations (>2000 m) giving a large accumulation of snow (Figure 8a).

The SWE accumulation is less and snow only lasts one day at lower elevations, and tends to zero below 1000 m, where all precipitation is in the form of rainfall (data not shown). This is a typical ROS event at low elevations, with snowfall at higher locations, due to the temperature decrease with elevation. In Figure 8b, the cumulative quantity of rainfall and snowmelt into the catchment per square meter, are shown. The precipitation event, and consequently the floods generated, were not equally intense across the catchments (see *Y* axis of panels and the return period of the flood event). Rainfall is the main driver of flood in all catchments, although snowmelt does contribute, as indicated by the R/S ratio. Unlike the contribution of rainfall, which reaches a peak that usually coincides with the time of peak flows, snowmelt usually keeps increasing after the peak flow. This is the reason why the floods with a contribution of snowmelt usually show larger duration and larger total flow values than *rain* events (Figure 5 and Section 3.2). Streamflow show a large increase starting on December 18, the exact same day that the peak flow occurred in the tributaries (Figure 8c). The baseflow before the flood event was about 250 m^3 s^{-1}, just a little below the mean annual flow of the river (~300 m^3 s^{-1}). A peak flow of 1400 m^3 s^{-1} is reached three days after the peak flow at the tributaries. The Ebro River constitutes the key axis of socio-economic development of northeast Spain. The Pyrenean tributaries are the main contributors to its annual streamflow [45], but they are also a source of flooding as we have demonstrated. Increasing knowledge on the triggering mechanisms of floods can help improving policies and management practices for minimizing the potential impact of the risk.

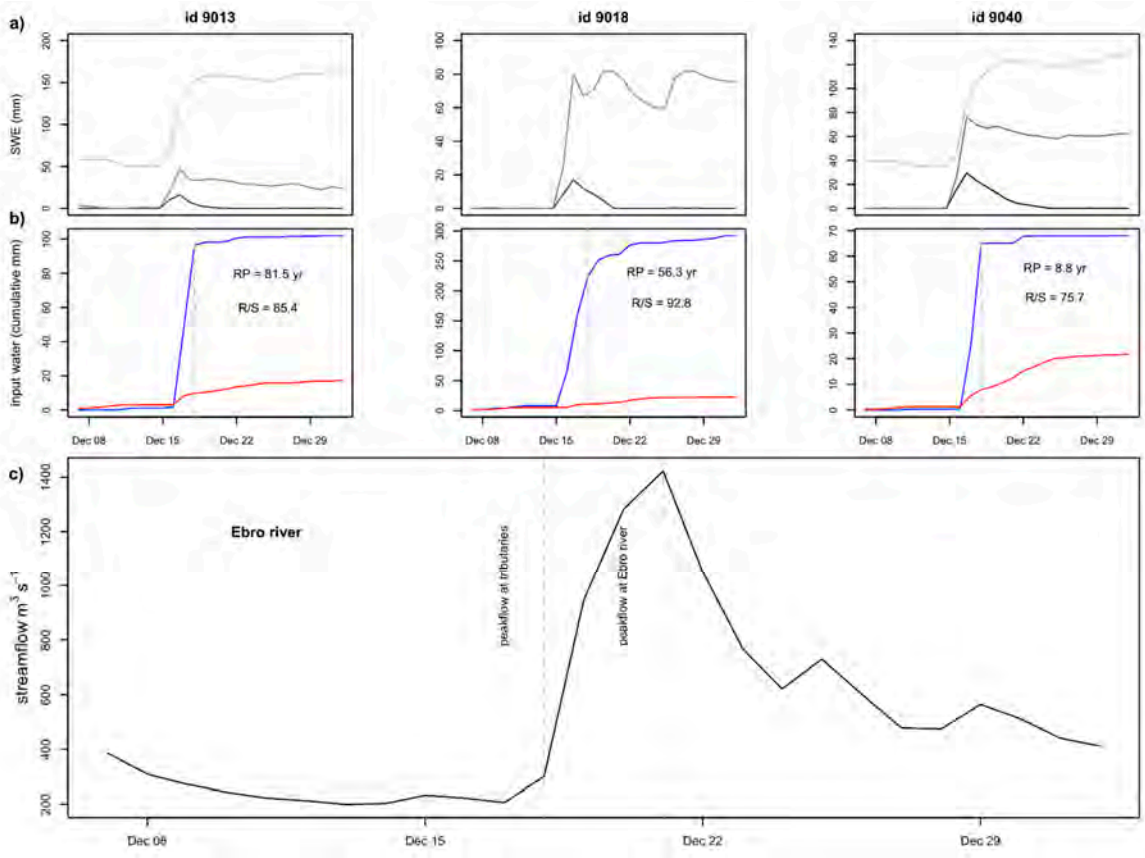

Figure 8. Example of mountain flood event at the Pyrenees and hydrological impact downstream. (**a**) snow water equivalent (SWE) accumulated on the catchment at different elevation bands: 1000 m (black line), 1500 m (grey line), and 2000 m (light grey line); (**b**) cumulative water input in the catchment per square meter as rainfall (blue line) and meltwater (red line). RP: return period of flood event; R/S: rain/snowmelt ratio. Dashed line indicates the day of peak flow. (**c**) The hydrological consequences of flooding from all 8 tributaries on the river discharge at the Ebro River (Zaragoza gauge station) during the event.

4. Discussions and Conclusions

Since flooding is the most important and frequent hazard in Spain [17], this study determines the influence of snowmelt on the generation of floods. We focused on mountain regions in order to separate the role of snowmelt from the rain, since this has not received much previous attention about flood initiation. This work does not examine the area of Spain with more frequent and violent flooding (the eastern region at the Mediterranean coast), since that type of flash-flooding in Mediterranean catchments has been extensively researched [22,23,46–50], and the role of snow in those areas is marginal or non-existent. The mountain rivers that were selected represent the entire mountain systems in which they are located (Figure 1). Most of the studied rivers, along with nearby rivers that could not be included in the study due to a lack of data, are tributaries of two of the major Spanish rivers, the Duero and the Ebro. These rivers cover a large area within Spain and have important economies and large populations that are exposed to high vulnerability when flooding occurs [19,51]. Floods in mountain catchments can occur in isolation when convective storms develop due to orography uplift, and produce destructive consequences at the local scale [52]. But when synoptic situations generate intense rainfall over large areas, floods can occur concurrently in different catchments located in the same mountain system. When this happens, the consequences of river flooding can extend beyond the local catchment and affect downstream areas as illustrated in the case study for the Pyrenean catchments (Section 3.5 and Figure 8).

In the Spanish mountains, rainfall triggers the majority of the studied floods (Figure 2a). The role of snowmelt (of about 18% weight on average) is usually limited to increase the duration of the receding limb after the peak flows are reached, and consequently the total amount of water involved in the flood, due to the gradual nature of the snowmelt process. Events where rainfall and snowmelt contributed similarly constitute about 20% of cases, while floods where snowmelt is the main contributor (*ROS_s* and *snow* floods) only constitute 5% of the events (Figure 2a). We must clarify here that these results reflect the method used for defining the R/S ratio and the subsequent characterization of floods. Such a ratio is considered as the relative amount of rainfall/snowmelt from the total cumulative water since the beginning of the event until the peak flow is reached. We selected the day of the peak flow due to its straightforward identification in the 250 hydrographs. Since the contribution of snowmelt usually continues after the peak flow, if we had used another time in the hydrograph for defining the R/S ratio, such as the end of the receding limb, the quantification of snowmelt in our results would have been larger. In general terms we observed that the contribution of snowmelt for generating floods was usually larger in catchments with lower temperatures, and larger snow accumulation (Figure 6). This, however, does not apply to the floods where snowmelt was the sole contributing factor (only 6 of the 250 events). These events seem to happen in mid-elevation catchments that may sporadically accumulate a large quantity of snow in mid-spring days, and once the cold event with accumulation ends, snow melts rapidly.

The majority of large floods in Spanish mountain rivers occurred in the winter months (specially December and January), and to a lesser extent in spring and fall with very few were occurring in the summer (Figure 4). This partially coincides with the observation of seasonality of large historical floods in the main Spanish rivers. Barriendos and Rodrigo [19] showed that floods in rivers draining to the Atlantic occurred primarily in winter, whereas in rivers draining to the Mediterranean flooding was more frequent in fall. This is related to the atmospheric patterns that lead to large rainfall amounts in the Iberian Peninsula. Atlantic basins are usually affected by southern and western flows that bring wet air masses and frontal systems from the Atlantic Ocean, governed by the North Atlantic Oscillation, with a more prominent intensity in winter [43,53–55]. Conversely, large rainfall amounts in the Mediterranean basins are more intense and concentrated in events of few hours, and have usually a convective origin, due to the concurrence of a cold depression in the middle troposphere (cut-off-low) with advection of warm flows from the Mediterranean [56]. Such is a typical situation in September and October months, and is associated with the generation of flash-floods.

Our investigation reveals that floods in mountain rivers can occur under any type of weather type, although cyclonic, and advection from SW–W and E–SE are the most dominant modes of surface circulation for flood occurrence (Figure 7). This is similar to the findings of Cortesi et al. [41] who demonstrated that most of the (monthly) precipitation on the Iberian Peninsula occurs under cyclonic and W and SW weather types with variations depending on the spatial context; in particular, advection from the East dominates precipitation in the Mediterranean coast, and flows from the North in the Cantabrian coast. There are no clear differences between the types of floods and the connection to the weather type (Figure 7a), although for floods with a presence of snowmelt, the advection from E and SE prevail (Figure 7b). When comparing floods and weather types as a function of mountain system, we observe that the geographical location of the mountain range, as well as the orientation with respect to prevailing winds (Figure 7c), affects the occurrence of floods. For example, in the Cantabrian range, located in Northern Spain (Figure 2), with a zonal configuration, prevailing weather types for triggering floods, aside from cyclonic circulation, are advection from the SW and SE (Figure 7c), corresponding to the rivers draining the south face of the mountain range, but also advection from NE and N, that triggers flooding in the rivers draining the north slopes. Conversely, the Iberian mountains, that are more exposed to eastern flows due to their geographical location and alignment (NW–SE), cyclonic and E advection are the dominant weather types for flood occurrence (Figure 7c). Likewise, in the Central System, that is sheltered from northern flows by the Cantabrian Mountains and the Duero River basin, the majority of floods occurred under advection from SE and SW. Anticyclonic circulation only accounts for 7% of the cases that generate floods, but it is particularly relevant in the Pyrenees and in the river located at the Baetic mountains. Anticyclonic circulation is the most common weather type in the Iberian Peninsula, but it shows the lower contribution to monthly precipitation [41] and yields only one-third of the floods as cyclonic circulation does (Figure 7a). The occurrence of intense rainfall leading to floods under these synoptic conditions may be explained by the capacity of high mountains for triggering convective processes at the local scale [57], or also by conditions in the middle troposphere (e.g., advection of a cut-off-low), that are not accounted for by the weather types approach used [41,58].

Mountains are, indeed, subject of more complex atmospheric mechanisms, and may combine both, frontal, and orographic precipitation. In the case of the mountain rivers in our study, floods in spring are common (Figure 4), and this is associated to the contribution of snowmelt. While *rain* events tend to occur more frequently in early winter days, floods with a contribution of snowmelt occur in late winter and early spring, and the more contribution of snow, the more advanced the spring (see Figure 4). This lies within normality, as snowmelt, and consequently nival peak flows in the Iberian Peninsula are at a maximum between March and June, depending on the mountain system or the elevation of the catchment [26–28]. Such flooding occurs 45% of the time, and falls within the definition of a ROS event, i.e., a precipitation event that occurs on a mountain slope with an existing snowpack, and depending on the elevation it may be solid or liquid. At high elevations it contributes to increase the quantity of snow, and at lower elevations it falls as rain on the snow surface. As zero degree isotherm increases in elevation, the more snow is available to melt and therefore the more intense that the ROS event will be. During a ROS, the addition of snowmelt water to the water from rainfall is an important contributor or even the triggering mechanism of floods in temperate and cold environments. Such is the case of mountains in North America [10,15,59], and the Alps [12], or the Pyrenees [14] in Europe. Moreover, the antecedent soil moisture is usually higher on snow-covered slopes from the infiltration of meltwater into the soil during the snow season, further facilitating the occurrence of a flood during a ROS event [11]. The quantity of rain falling on the snow surface does not automatically trigger snowmelt since the high latent heat necessary for snow to melt (79.7 cal g^{-1} at 0 °C) is much higher than the specific heat of water (1 cal g^{-1} $°C^{-1}$), thus rainfall must be very intense for this to occur. For snowpack to melt during a ROS, in addition to the energy advected by rain, it is necessary the contribution from turbulent sensible and latent heat transfer associated with condensation and sublimation under saturated conditions and with high air and dew

point temperatures [15,60,61]. Some of the big precipitation events in the Iberian Peninsula occur as atmospheric rivers [62] and these may bring moist air that substantially increases longwave radiation that enhances snowmelt [63]. Since our research focused on the regional characteristics of flooding, we did not explore the energy balance components of the snowpack during the flood events. Further research considering physical approaches on a finer scale should investigate the role that variables such as temperature, relative humidity or solar radiation may play on the occurrence of ROS triggered floods in the Spanish mountains.

Our investigation constitutes the first research about ROS events in Spain at a large scale. Our results reveal that this type of hydro-meteorological event is far from being rare in the mountains of this country. Even if the extension of snow cover in Spain is not comparable to countries at higher latitudes, and the persistent seasonal snowpack is confined to the highest mountain areas (generally above 1500 m a.s.l. [24]), it affects downstream areas and can be a potential source of risk for populations. Increasing temperatures in recent decades, and projected climate warming are considered to induce changes in the spatial and temporal frequency of ROS events. For example, Beniston and Stoffel [12] observed an increase in the number of ROS in an alpine catchment due to regional warming over the last five decades and projected a likely increase with future IPCC warming projections up to 4 °C; more temperature warming would probably lead to a decrease in the number of ROS. Likewise, Surfleet and Tullos [10] projected an increase in the number of ROS associated peak flows under future climate warming in Oregon (USA), although the frequency of high peak flows triggered by ROS in middle elevation zones would decrease. Contrasting results are as well found, such as Leung et al. [64] who observed an increase in the frequency of ROS events during winter for the Columbia River basin (western USA), but projected fewer ROS events under future warmer conditions due to a shorter duration of snowpack. Further, Morán-Tejeda et al. [16] pointed to a seasonal and elevation dependence of the frequency of ROS with changing temperatures in the Swiss Alps, which controls the trade-off between the duration of the snowpack and the elevation of the transient snow-rain zone over the year for a ROS to happen. All these findings confirm the necessity to explore the spatio–temporal frequency of ROS in the Spanish mountains and its implication for water and risk management under changing climate conditions.

Author Contributions: Conceptualization, E.M.-T., S.R.F. and J.L.-L.; methodology, E.M.-T., S.R.F., J.I.L.-M. and C.G.; data curation and validation, E.M.-T. and E.A.-G.; formal analysis, E.M.-T., S.R.F., J.L.-L. and A.-J.C.-L.; writing—original draft preparation, E.M.-T.; writing—review and editing, S.R.F., J.I.L.-M., C.G., J.L.-L., A.-J.C.-L.; funding acquisition, J.I.L.-M. and E.M.-T.

Funding: This Project has been funded with HIDROIBERNIEVE Project (CGL2017-82216-R) by the Ministry of Science, Innovation and Universities. Author EMT was founded by Ministry of Education, Science and Sport, through the program Programa Estatal de Promoción y Talento y su Empleabilidad en I+D+I, Subprograma Estatal de Movilidad, del Plan Estatal de Investigación Científica y Técnica y de Innovación 2013–2016.

Acknowledgments: EMT acknowledges the Watershed Science Program, Department of Ecosystem Science and Sustainability, and the Natural Resource Ecology Laboratory of the Colorado State University for hosting him during the winter of 2018–2019.

Conflicts of Interest: The authors declare no conflict of interest. The funders had no role in the design of the study; in the collection, analyses, or interpretation of data; in the writing of the manuscript, or in the decision to publish the results.

References

1. Viviroli, D.; Dürr, H.H.; Messerli, B.; Meybeck, M.; Weingartner, R. Mountains of the world, water towers for humanity: Typology, mapping, and global significance. *Water Resour. Res.* **2007**, *43*. [CrossRef]
2. Houze, R.A. Orographic effects on precipitating clouds. *Rev. Geophys.* **2012**, *50*, RG1001. [CrossRef]
3. Bodoque, J.M.; Díez-Herrero, A.; Eguibar, M.A.; Benito, G.; Ruiz-Villanueva, V.; Ballesteros-Cánovas, J.A. Challenges in paleoflood hydrology applied to risk analysis in mountainous watersheds—A review. *J. Hydrol.* **2015**, *529*, 449–467. [CrossRef]

4. Weingartner, R.; Barben, M.; Spreafico, M. Floods in mountain areas—An overview based on examples from Switzerland. *J. Hydrol.* **2003**, *282*, 10–24. [CrossRef]
5. Zeinivand, H.; De Smedt, F. Prediction of snowmelt floods with a distributed hydrological model using a physical snow mass and energy balance approach. *Nat. Hazards* **2010**, *54*, 451–468. [CrossRef]
6. Cunderlik, J.M.; Ouarda, T.B.M.J. Trends in the timing and magnitude of floods in Canada. *J. Hydrol.* **2009**, *375*, 471–480. [CrossRef]
7. Marks, D.; Kimball, J.; Tingey, D.; Link, T. The sensitivity of snowmelt processes to climate conditions and forest cover during rain-on-snow: A case study of the 1996 Pacific Northwest flood. *Hydrol. Process.* **1998**, *12*, 1569–1587. [CrossRef]
8. McCabe, G.J.; Clark, M.P.; Hay, L.E.; McCabe, G.J.; Clark, M.P.; Hay, L.E. Rain-on-Snow Events in the Western United States. *Bull. Am. Meteorol. Soc.* **2007**, *88*, 319–328. [CrossRef]
9. Kattelmann, R.F. Flooding from Rain-on-Snow Events in the Sierra Nevada. In *Proceedings of the North American Water and Environment Congress & Destructive Water (ASCE)*; Bathala, C., Ed.; International Association of Hydrological Sciences: Wallingford, UK, 1996.
10. Surfleet, C.G.; Tullos, D. Variability in effect of climate change on rain-on-snow peak flow events in a temperate climate. *J. Hydrol.* **2013**, *479*, 24–34. [CrossRef]
11. Sui, J.; Koehler, G. Rain-on-snow induced flood events in Southern Germany. *J. Hydrol.* **2001**, *252*, 205–220. [CrossRef]
12. Beniston, M.; Stoffel, M. Rain-on-snow events, floods and climate change in the Alps: Events may increase with warming up to 4 °C and decrease thereafter. *Sci. Total Environ.* **2016**, *571*, 228–236. [CrossRef] [PubMed]
13. Merz, R.; Blöschl, G. A process typology of regional floods. *Water Resour. Res.* **2003**, *39*. [CrossRef]
14. Corripio, J.; López-Moreno, J. Analysis and Predictability of the Hydrological Response of Mountain Catchments to Heavy Rain on Snow Events: A Case Study in the Spanish Pyrenees. *Hydrology* **2017**, *4*, 20. [CrossRef]
15. Pomeroy, J.W.; Fang, X.; Marks, D.G. The cold rain-on-snow event of June 2013 in the Canadian Rockies—Characteristics and diagnosis. *Hydrol. Process.* **2016**, *30*, 2899–2914. [CrossRef]
16. Morán-Tejeda, E.; López-Moreno, J.; Stoffel, M.; Beniston, M. Rain-on-snow events in Switzerland: Recent observations and projections for the 21st century. *Clim. Res.* **2016**, *71*, 111–125. [CrossRef]
17. Pujadas-Ferrer, J. Las inundaciones en España: Impacto económico y gestión del riesgo. In *Riesgos Naturales*; Ayala-Carcedo, F.J., Olcina, J., Eds.; Ariel Ciencia: Barcelona, Spain, 2002; pp. 879–888.
18. European Environment Agency. *Flood Risks and Environmental Vulnerability Exploring the Synergies between Floodplain Restoration, Water Policies and Thematic Policies*; Publications Office of the European Union: Luxembourg, 2016; ISBN 9789292137168.
19. Barriendos, M.; Rodrigo, F.S. Study of historical flood events on Spanish rivers using documentary data. *Hydrol. Sci. J.* **2006**, *51*, 765–783. [CrossRef]
20. Camarasa-Belmonte, A.M. Crecidas e inundaciones. In *Riesgos Naturales*; Ayala-Carcedo, F.J., Olcina, J., Eds.; Ariel Ciencia: Barcelona, Spain, 2002; pp. 859–879.
21. Marchi, L.; Borga, M.; Preciso, E.; Gaume, E. Characterisation of selected extreme flash floods in Europe and implications for flood risk management. *J. Hydrol.* **2010**, *394*, 118–133. [CrossRef]
22. Llasat, M.C.; Llasat-Botija, M.; Prat, M.A.; Porcú, F.; Price, C.; Mugnai, A.; Lagouvardos, K.; Kotroni, V.; Katsanos, D.; Michaelides, S.; et al. High-impact floods and flash floods in Mediterranean countries: The FLASH preliminary database. *Adv. Geosci.* **2010**, *23*, 47–55. [CrossRef]
23. Lara, A.; Saurí, D.; Ribas, A.; Pavón, D. Social perceptions of floods and flood management in a Mediterranean area (Costa Brava, Spain). *Nat. Hazards Earth Syst. Sci.* **2010**, *10*, 2081–2091. [CrossRef]
24. Alonso-González, E.; López-Moreno, J.I.; Navarro-Serrano, F.; Sanmiguel-Vallelado, A.; Revuelto, J.; Domínguez-Castro, F.; Ceballos, A. Snow climatology for the mountains in the Iberian Peninsula using satellite imagery and simulations with dynamically downscaled reanalysis data. *Int. J. Climatol.* **2019**. [CrossRef]
25. Herrero, J.; Polo, M.J.; Losada, M.A. Snow evolution in Sierra Nevada (Spain) from an energy balance model validated with Landsat TM data. In *Remote Sensing for Agriculture, Ecosystems, and Hydrology XIII*; Neale, C.M.U., Maltese, A., Eds.; International Society for Optics and Photonics: Bellingham, DC, USA, 2011; Volume 8174, p. 817403.

26. López-Moreno, J.I.; García-Ruiz, J.M. Influence of snow accumulation and snowmelt on streamflow in the central Spanish Pyrenees / Influence de l'accumulation et de la fonte de la neige sur les écoulements dans les Pyrénées centrales espagnoles. *Hydrol. Sci. J.* **2004**, *49*. [CrossRef]
27. Morán-Tejeda, E.; Lorenzo-Lacruz, J.; López-Moreno, J.I.; Rahman, K.; Beniston, M. Streamflow timing of mountain rivers in Spain: Recent changes and future projections. *J. Hydrol.* **2014**, *517*, 1114–1127. [CrossRef]
28. Sanmiguel-Vallelado, A.; Morán-Tejeda, E.; Alonso-González, E.; López-Moreno, J.I. Effect of snow on mountain river regimes: An example from the Pyrenees. *Front. Earth Sci.* **2017**, *11*, 515–530. [CrossRef]
29. López-Moreno, J.I.; Revuelto, J.; Fassnacht, S.R.; Azorín-Molina, C.; Vicente-Serrano, S.M.; Morán-Tejeda, E.; Sexstone, G.A. Snowpack variability across various spatio-temporal resolutions. *Hydrol. Process.* **2015**, *29*, 1213–1224. [CrossRef]
30. Gil, F.E. Hacia una clasificación de las situaciones de inundación en la cuenca del Ebro, en función de sus causas atmosféricas. *Geographicalia* **2008**, *53*, 73–100.
31. Serrano-Notivoli, R.; Mora Mur, D.; Ollero Ojeda, A.; Sánchez Fabre, M.; Saz Sánchez, M.Á. Respuesta hidrológica al evento de precipitación de Junio de 2013 en el Pirineo Central. *Investigaciones Geográficas* **2014**, *62*, 5–21. [CrossRef]
32. Alonso-González, E.; López-Moreno, J.I.; Gascoin, S.; García-Valdecasas Ojeda, M.; Sanmiguel-Vallelado, A.; Navarro-Serrano, F.; Revuelto, J.; Ceballos, A.; Esteban-Parra, M.J.; Essery, R. Daily gridded datasets of snow depth and snow water equivalent for the Iberian Peninsula from 1980 to 2014. *Earth Syst. Sci. Data Discuss.* **2018**, 1–24. [CrossRef]
33. Centro de Estudios Hidrográficos. Available online: http://ceh-flumen64.cedex.es/general/default.htm (accessed on 8 September 2018).
34. García-Valdecasas Ojeda, M.; Gámiz-Fortis, S.R.; Castro-Díez, Y.; Esteban-Parra, M.J. Evaluation of WRF capability to detect dry and wet periods in Spain using drought indices. *J. Geophys. Res. Atmos.* **2017**, *122*, 1569–1594. [CrossRef]
35. Singh, V.P. Generalized Extreme Value Distribution. In *Entropy-Based Parameter Estimation in Hydrology*; Water Science and Technology Library; Springer: Dordrecht, The Nezerlands, 1998; pp. 169–183.
36. Morrison, J.E.; Smith, J.A. Stochastic modeling of flood peaks using the generalized extreme value distribution. *Water Resour. Res.* **2002**, *38*, 41. [CrossRef]
37. Harder, P.; Pomeroy, J. Estimating precipitation phase using a psychrometric energy balance method. *Hydrol. Process.* **2013**, *27*, 1901–1914. [CrossRef]
38. Trigo, R.M.; DaCamara, C.C. Circulation weather types and their influence on the precipitation regime in Portugal. *Int. J. Climatol.* **2000**, *20*, 1559–1581. [CrossRef]
39. Jenkinson, A.F.; Collison, F.P. An initial climatology of Gales over the North Sea. In *Synoptic Climatology Branch Memorandum*; Meteorological Office: Bracknell, UK, 1977; Volume 62.
40. Jones, P.D.; Hulme, M.; Briffa, K.R. A comparison of Lamb circulation types with an objective classification scheme. *Int. J. Climatol.* **1993**, *13*, 655–663. [CrossRef]
41. Cortesi, N.; Gonzalez-Hidalgo, J.C.; Trigo, R.M.; Ramos, A.M. Weather types and spatial variability of precipitation in the Iberian Peninsula. *Int. J. Climatol.* **2014**, *34*, 2661–2677. [CrossRef]
42. Paredes, D.; Trigo, R.M.; Garcia-Herrera, R.; Trigo, I.F.; Paredes, D.; Trigo, R.M.; Garcia-Herrera, R.; Trigo, I.F. Understanding Precipitation Changes in Iberia in Early Spring: Weather Typing and Storm-Tracking Approaches. *J. Hydrometeorol.* **2006**, *7*, 101–113. [CrossRef]
43. Goodess, C.M.; Jones, P.D. Links between circulation and changes in the characteristics of Iberian rainfall. *Int. J. Climatol.* **2002**, *22*, 1593–1615. [CrossRef]
44. Cortesi, N.; Trigo, R.M.; Gonzalez-Hidalgo, J.C.; Ramos, A.M. Modelling monthly precipitation with circulation weather types for a dense network of stations over Iberia. *Hydrol. Earth Syst. Sci.* **2013**, *17*, 665–678. [CrossRef]
45. López-Moreno, J.I.; Beniston, M.; García-Ruiz, J.M. Environmental change and water management in the Pyrenees: Facts and future perspectives for Mediterranean mountains. *Glob. Planet. Chang.* **2008**, *61*, 300–312. [CrossRef]
46. Llasat, M.C.; Marcos, R.; Llasat-Botija, M.; Gilabert, J.; Turco, M.; Quintana-Seguí, P. Flash flood evolution in North-Western Mediterranean. *Atmos. Res.* **2014**, *149*, 230–243. [CrossRef]
47. Llasat, M.C.; López, L.; Barnolas, M.; Llasat-Botija, M. Flash-floods in Catalonia: The social perception in a context of changing vulnerability. *Adv. Geosci.* **2008**, *17*, 63–70. [CrossRef]

48. Barnolas, M.; Llasat, M.C. A flood geodatabase and its climatological applications: The case of Catalonia for the last century. *Nat. Hazards Earth Syst. Sci.* **2007**, *7*, 271–281. [CrossRef]
49. Llasat, M.-C.; Barriendos, M.; Barrera, A.; Rigo, T. Floods in Catalonia (NE Spain) since the 14th century. Climatological and meteorological aspects from historical documentary sources and old instrumental records. *J. Hydrol.* **2005**, *313*, 32–47. [CrossRef]
50. Bull, L.; Kirkby, M.; Shannon, J.; Hooke, J. The impact of rainstorms on floods in ephemeral channels in southeast Spain. *Catena* **2000**, *38*, 191–209. [CrossRef]
51. Espejo, F.; Domenech, S.; Ollero, A.; Sánchez, M. *Boletín de la Asociación de Geógrafos Españoles*; AGE: Madrid, Spain, 2008.
52. White, S.; García-Ruiz, J.M.; Martí, C.; Valero, B.; Errea, M.P.; Gómez-Villar, A. The 1996 Biescas campsite disaster in the Central Spanish Pyrenees, and its temporal and spatial context. *Hydrol. Process.* **1997**, *11*, 1797–1812. [CrossRef]
53. Morán-Tejeda, E.; López-Moreno, J.; Ceballos-Barbancho, A.; Vicente-Serrano, S.M. Evaluating Duero's basin (Spain) response to the NAO phases: Spatial and seasonal variability. *Hydrol. Process.* **2011**, *25*, 1313–1326. [CrossRef]
54. Trigo, R.M.; Pozo-Vázquez, D.; Osborn, T.J.; Castro-Díez, Y.; Gámiz-Fortis, S.; Esteban-Parra, M.J. North Atlantic oscillation influence on precipitation, river flow and water resources in the Iberian Peninsula. *Int. J. Climatol.* **2004**, *24*, 925–944. [CrossRef]
55. Muñoz-Diaz, D.; Rodrigo, F.S. Spatio-temporal patterns of seasonal rainfall in Spain (1912–2000) using cluster and principal component analysis: Comparison. *Ann. Geophys.* **2004**, *22*, 1435–1448. [CrossRef]
56. Romero, R.; Sumner, G.; Ramis, C.; Genovés, A. A classification of the atmospheric circulation patterns producing significant daily rainfall in the Spanish Mediterranean area. *Int. J. Climatol.* **1999**, *19*, 765–785. [CrossRef]
57. Wulfmeyer, V.; Behrendt, A.; Bauer, H.-S.; Kottmeier, C.; Corsmeier, U.; Blyth, A.; Craig, G.; Schumann, U.; Hagen, M.; Crewell, S.; et al. THE CONVECTIVE AND OROGRAPHICALLY INDUCED PRECIPITATION STUDY: A Research and Development Project of the World Weather Research Program for Improving Quantitative Precipitation Forecasting in Low-Mountain Regions. *Bull. Am. Meteorol. Soc.* **2008**, *89*, 1477–1486.
58. Nieto, R.; Gimeno, L.; De la Torre, L.; Ribera, P.; Barriopedro, D.; García-Herrera, R.; Serrano, A.; Gordillo, A.; Redaño, A.; Lorente, J. Interannual variability of cut-off low systems over the European sector: The role of blocking and the Northern Hemisphere circulation modes. *Meteorol. Atmos. Phys.* **2007**, *96*, 85–101. [CrossRef]
59. Fassnacht, S.R.; Records, R.M. Large snowmelt versus rainfall events in the mountains. *J. Geophys. Res. Atmos.* **2015**, *120*, 2375–2381. [CrossRef]
60. Mazurkiewicz, A.B.; Callery, D.G.; McDonnell, J.J. Assessing the controls of the snow energy balance and water available for runoff in a rain-on-snow environment. *J. Hydrol.* **2008**, *354*, 1–14. [CrossRef]
61. Marks, D.; Link, T.; Winstral, A.; Garen, D. Simulating snowmelt processes during rain-on-snow over a semi-arid mountain basin. *Ann. Glaciol.* **2001**, *32*, 195–202. [CrossRef]
62. Ramos, A.M.; Trigo, R.M.; Liberato, M.L.R.; Tomé, R.; Ramos, A.M.; Trigo, R.M.; Liberato, M.L.R.; Tomé, R. Daily Precipitation Extreme Events in the Iberian Peninsula and Its Association with Atmospheric Rivers*. *J. Hydrometeorol.* **2015**, *16*, 579–597. [CrossRef]
63. Curry, C.L.; Islam, S.U.; Zwiers, F.W.; Déry, S.J. Atmospheric Rivers Increase Future Flood Risk in Western Canada's Largest Pacific River. *Geophys. Res. Lett.* **2019**, *46*, 1651–1661. [CrossRef]
64. Leung, L.R.; Qian, Y.; Bian, X.; Washington, W.M.; Han, J.; Roads, J.O. Mid-Century Ensemble Regional Climate Change Scenarios for the Western United States. *Clim. Chang.* **2004**, *62*, 75–113. [CrossRef]